Conference Proceedings

EuroSun 2016
Palma de Mallorca (Spain), 11 - 14 October 2016

Optimizing design of a Linear Fresnel Reflector for process heat supply

Diego Pulido Iparraguirre[1, 2], Juan J. Serrano-Aguilera[1], Loreto Valenzuela[1] and Aránzazu Fernández-García[1]

[1] Plataforma Solar de Almería (CIEMAT-PSA), Spain

[2] Centro de Desarrollo Energético Antofagasta (CDEA), Universidad de Antofagasta (UA), Chile

Abstract

Lineal Fresnel Reflectors (LFR) is a promising technology in the field of concentrating solar thermal collectors which presents several advantages in comparison with the widely used parabolic-trough collectors (PTC). A methodology to properly design a LFR is presented as well as several issues arisen out the study of a particular case. As first step, a brief review was performed to select the proper receiver configuration, resulting in a trapezoidal cavity with multitube absorber receiver. Secondly, several stages of the optimized process were followed using an in-house ray tracer computer code to simulate the optical behavior of the system. Different characteristics, as width of the mirrors, number of rows, mirror geometry profile, height, length and configuration of the receiver, were optimized setting the power impinging in the absorber tube surface as the objective function. According to the results obtained, the shape of the mirrors was stablished based on the optical advantages that parabolic mirrors have over flatted ones. The point strategy was focused on achieving a homogeneous flux in the receiver tubes surface. The height of the receiver over the mirrors plane was selected as the one that maximizes the impinging power. A practical analysis related with the facilities characteristics was carried out to set the number and width of mirrors. In addition, a thermal balance between the impinging power and the thermal energy gained by the heat transfer fluid (HTF) was performed to calculate the length of the receiver tubes. Finally, the results of the analytical model were cross checked with a ray tracer software (Tonatiuh), with satisfactory results.

Keywords: *Lineal Fresnel Reflector, ray tracer, multitube absorber, point strategy.*

1. Introduction

LFR is a promising technology in the field of concentrating solar thermal collectors (Singh et al. 1999). The operating principle relays on a set of long and narrow mirrors that might be flat or slightly curved, which reflect direct solar radiation by tracking the sun along the day. The reflected solar beams are absorbed by a fixed receiver, which is the key component of the system. The energy absorbed by the receiver is transferred to the HTF circulating inside it, which increases its enthalpy. Several designs of receivers are found in the literature (Zhu et al. 2014), including receiver tubes arranged individually or in group protected from the ambient by a cover in order to minimize heat loses.

PTC are the main technology in terms of number of plants installed and currently in operation (Fernandez-Garcia et al. 2010), mostly because of the optimum results of SEGS plants in Mojave Desert, California, which are being producing electricity since the 80's until now. It has been found that LFR technology presents some significant advantages compared with PTC (Sahoo et al. 2012; Sait et al. 2015). On one hand, the costs of the optical components is lower in LFR, according to the nearly flat shape of the mirrors (Boito & Grena 2016) and also the absence of metal-glass welds in the receiver tubes, because in most of the designs the receiver tubes are not directly exposed to the ambient and no vacuum is needed. On the other hand, as the receiver is fixed, they do not use ball joints, as PTC does, at the points where the distribution pipe meets the start and end of the collector. As a consequence of this, lower maintenance and operation costs for LFR plants is achieved (Haeberle et al. 2002).

Selection and/or peer review under responsibility of Scientific Committee
doi:10.18086/eurosun.2016.02.21 Available at http://proceedings.ises.org

On the contrary, the main disadvantage of LFR compared with PTC, is the lower optical efficiency, explained by the longitudinal component of the radiation impinging the receiver's tubes, which increases when sun is far away from the zenithal position. Also, significant optical errors due to the large distance between the mirrors and the focal point contribute to decrease the optical performance (Boito & Grena 2016).

The receiver of a LFR may be considered as the most relevant component of the system because it is the place where the energy conversion process occurs. Its geometrical and optical configuration has changed, depending mainly on the application. Previously, the most common design was based on a single tube with a secondary reflector (see Fig. 1 left). This design could be conceived with a second glass tube surrounding the metal one and vacuum between both, or just a single steel tube with a glass flat cover sealing the receiver from outside climate conditions (Montes et al. 2016). Recent designs agree in using a trapezoidal cavity with a multitube absorber (see Fig. 2 right). The main advantages of trapezoidal cavity with multitube absorber are a higher efficiency in the transfer process and a more flexible design leading to simpler control of the flow through the tubes (Abbas et al. 2012).

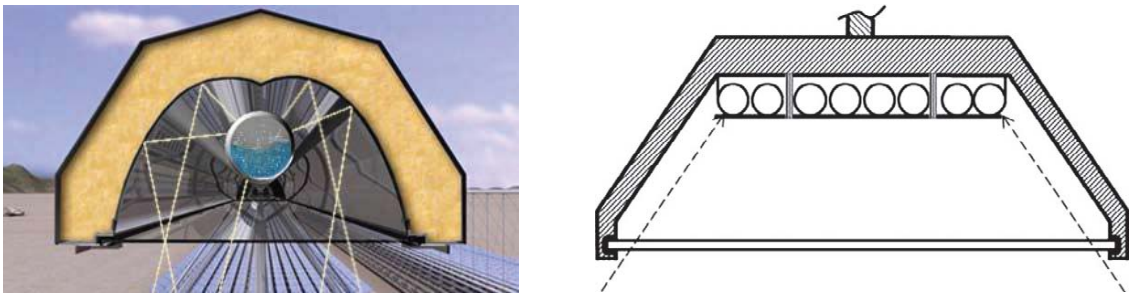

Fig. 1: Left: Single tube receiver configuration (source: Novatec Solar). Right: Trapezoidal cavity with multitube absorber receiver (source: Abbas et al. 2012).

Although the thermal energy consumption in industrial processes is significantly high (Kalogirou 2003) and LFR represents an economically feasible and clean solution, this technology is not as mature as expected. This paper presents a methodology to optimize the design of a LFR oriented to production of thermal energy for industrial process heat (IPH) applications at temperatures up to 200 ºC.

2. Methodology

This section includes the methodology followed in the design process of a LFR prototype for IPH applications. Different characteristics, as width of the mirrors, number of rows, mirror geometry profile, height, length and configuration of the receiver, were optimized, setting the power impinging in the absorber tube surface as the objective function.

2.1. Ray tracer

An in-house ray tracer computer code based on a Monte Carlo stochastic method developed in Matlab® was created (see the algorithm steps in Fig. 2), in order to study different configurations and geometries of the LFR prototype. This code gives the possibility to choose the Sunshape distribution from Buie, Neumann or Pillbox (Buie et al. 2003; Neumann et al. 2002). As a second step, an accumulated distribution function was obtained.

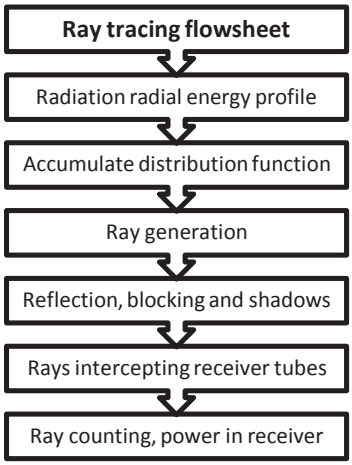

Fig. 2: Ray tracer flowsheet scheme.

A two-dimensional design was considered, in order to minimize the computing time of the simulations, folding the longitudinal coordinates into transversal plane and using a proper variable change. With this approach, the number of equations and variables was considerably reduced. This method does not disregard the longitudinal component of the impinging radiation, though. It involves a significant advantage because in case only the transversal component of the rays were considered, the path of the rays reflected from the mirror to the receiver would be considerably shorter than the path of those rays with longitudinal component.

In the rays path, reflection, blocking and shading are considered before the rays reach (or miss) the receiver surface. The rays that intercept the receiver tubes are then counted, given a power value assigned of each ray. Then, the concentrated flux profile on the receiver ($f(\theta)$) is calculated. The whole power impinging on the receiver is simply the sum of all of them, as indicated in equation (1).

$$q_t = \sum_{i=1}^{n} \int_{-\pi}^{\pi} r_{abs,i} \cdot f_i(\theta) \cdot d\theta \qquad \text{(eq. 1)}$$

where q_t [Wm^{-1}] is the sum of the power impinging in the *n* receiver tubes, $r_{abs,i}$ [m] is the radius of the tubes, and $f_i(\theta)$ [Wm^{-2}] is a function of the power received in every differential of the angular direction of the tube, θ.

Several simulations were done to develop an optimized design of a LFR. As base case, the code was run by using the meteorological data and the sun position of the *Plataforma Solar de Almería* (southern Spain). Five hours before and after noon were utilized for the simulations of one day from every month of the year. The power impinging in the receiver was maximized, and the geometry of the LFR that achieves this maximum was accepted as the optimal design.

2.2. Receiver configuration

The first step followed to select the receiver configuration for the LFR under design was to perform a literature revision, taking into consideration the operating conditions of the industrial process where the LFR designed will be used. The trapezoidal cavity with a multi-tube receiver was selected as the proper configuration (see section 3.1) and the number of tubes was set.

2.3. Shape of mirrors

Once the receiver configuration was chosen, the next step was to select the shape of the concentrating mirrors. The possibilities were restricted to flat shape or parabolic shape due to practical and economic issues. The analysis was made by simulating the power impinging in the receiver for both alternative shapes.

As shown in Fig. 3a, the image reflected by flat mirrors on the receiver, w_r, is approximately equivalent to the width of the mirrors, w_1 ($w_1 \approx w_r$). That is, the distance traveled by the reflected rays from the mirror to the receiver will not considerably increase the final width of the image at the receiver surface. For this reason, the optimal width for flat shaped mirrors should be close to the width of the receiver, w_R ($w_r \approx w_R$). If this condition was not stablished and wider mirrors were used (with a width of w_2, being $w_2 > w_1$ as displayed in Fig. 3b), the reflected image would certainly be wider than the receiver ($w_r > w_R$) and several rays will miss the target.

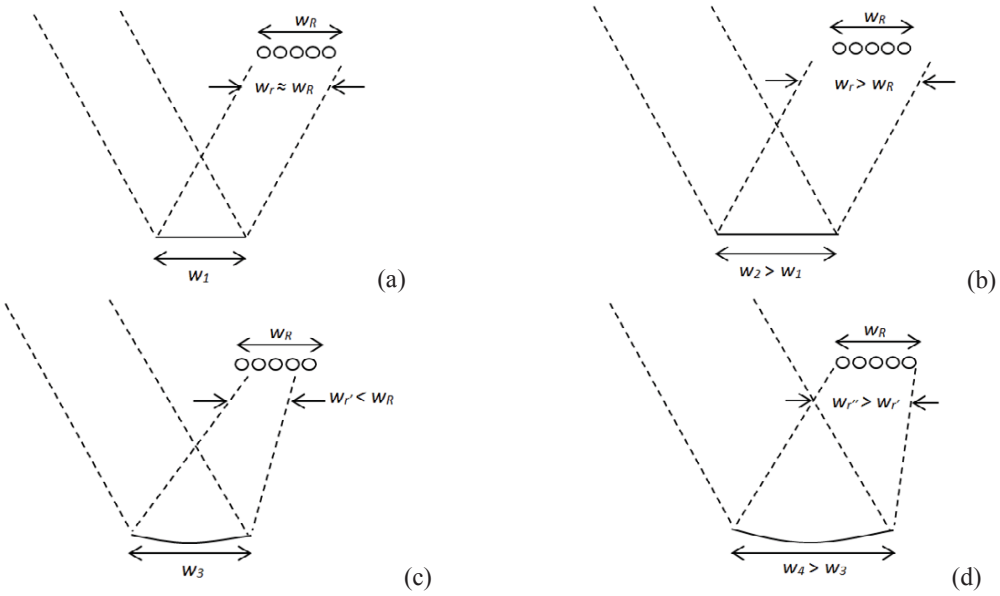

Fig. 3: Schemes representing the influence of the width in flat and parabolic shaped mirrors in the image reflected over the receiver.

In case of using parabolic mirrors (with a certain width, w_3), the image reflected by the mirrors will tend to converge to the focal point of the parabola, reflecting a beam of rays whose width ($w_{r'}$) is lower than the receiver width, $w_{r'} < w_R$ (Fig. 3c). In order to increase the power impinging into the receiver, wider mirrors ($w_4 > w_3$) could be considered without the limitation found in flat shaped mirrors. Wider mirrors imply more radiation in the reflector aperture ($w_{r''} > w_{r'}$), which leads to raise the concentration factor of the LFR (Fig. 3d). In addition, the height of the receiver over the lines of mirrors must be adjusted in order to fit the image reflected to the target.

2.4. Point strategy

The point strategy, i.e. the image that reflected rays form in the receiver transversal surface, has a significant relevance in the overall performance of LFR. Due to the fact that the receiver is not a singular aiming point, but a group of tubes, every tube should be lightened homogeneously. In other words, a homogeneous flux should be maintained so that hot spot which could lead to thermal stress in the tube material can be avoided. Several point strategies were analyzed with the in-house ray-tracing simulation code in order to address this issue along with the concentration ratio.

2.5. Height of the receiver

The distance from the mirrors plane to the receiver was established by maximizing the power delivered to the receiver. A set of calculations for different heights, fixing the rest of parameters, was carried out to study the relationship among the different geometrical parameters and to find the combination that yields an optimum height.

2.6. Number and width of mirrors

Having on goal the collection of maximum power, the selection of the number and width of mirrors is not a trivial issue. More and wider mirrors imply a larger reflecting surface which leads to more solar radiation collected in the aperture of the LFR. As a consequence, the power maximization cannot be the only design criterion to find the optimum number and width of mirrors. An economical approach combined with practical and technical aspects of the industrial facilities, where this system will be installed, is the best strategy to follow.

2.7. Length of receiver tubes

When the rest of the parameters explained in the previous sections were selected and the power in the receiver was obtained by the software developed, the next step was to simulate the thermal behavior of the receiver to calculate the tubes length required to achieve a certain increase of HTF temperature. In LFR technology,

thermal losses from tubes to ambient are mostly governed by radiation effect, having the convection mechanism a lower influence, and the conduction phenomena a negligible contribution (Pye et al. 2003; Singh et al. 2010). Different authors (Kumar et al. 2012; Reynolds et al. 2002; Sahoo et al. 2012) have developed experimental correlations for the same receiver configuration selected in this work. They consider the Nusselt number (see eq. 2) as the principal parameter to study the thermal losses due to both radiation and convection from the tubes to the glass cover window. The correlations given by these three studies mentioned were analyzed and compared among them.

$$Nu_{\sigma+h} = \frac{q_{\sigma+h} \cdot D}{k_f \cdot (T_{abs} - T_{cov})} \qquad \text{(eq. 2)}$$

where $Nu_{\sigma+h}$ [-] is the overall Nusselt number that regards radiation and convection effect, $q_{\sigma+h}$ [Wm^{-2}] is the overall heat flux, D [m] is the distance from the tubes to the glass cover window, k_f [$Wm^{-1}K^{-1}$] is the thermal conductivity of the fluid, T_{abs} [K] is the temperature of the tubes and T_{cov} [K] is the temperature of the glass cover window.

Additionally, a fourth correlation, in which a theoretical approach is made, was included in the study. This theoretical approach considers two flat parallel plates (Incropera, 2007). The hot one (simulating the tubes) is located above and facing down and the cold one (simulating the glass cover) is situated below. The equations ruling this condition respond to external free convection flows over horizontal plates.

3. Results

The results obtained in the LFR design process by using the in-house software developed in this work are presented in this section. This results belong to particular requirement stablished, however the process could be followed by any other set of conditions.

3.1. Receiver configuration

The final receiver configuration selected was based on the information collected from the literature along with the operating conditions of the industrial process to be supplied, i.e. thermal energy demand, fluid temperature and mass flow rate. A trapezoidal cavity with a multitube absorber design presents the best operation condition in terms of flow control alongside the simplicity of the receiver assembly. After considering several configurations (ranging from 2 to 8 tubes), the design option chosen incorporates 6 parallels tubes. This design is flexible and allows restricting the flow to central tubes, if radiation is lower than a certain value, in order to maintain a stable operation temperature.

3.2. Shape of mirrors

A comparison of the power impinging in the receiver was made between parabolic and flat shaped mirrors (see section 2.3). An increase in the width of the mirrors delivered similar results for both options until mirrors reach the same width of the receiver, w_R (see Fig. 4). For mirror widths higher than w_R, the increase of this parameter leads to directly enhance the power for the parabolic shape. However, the flat shape does not respond in the same way because of the overflow effect previously explained. According to these results, the parabolic shaped mirrors are preferred instead of flat shaped mirrors.

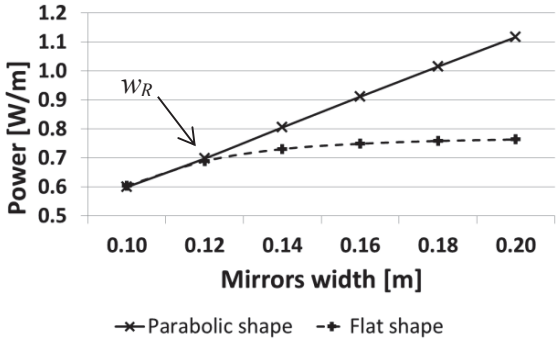

Fig. 4: Normalized power ($Power_{reference}$ = 1 Wm^{-2}) in the receiver according to the width of flat and parabolic shaped mirrors. For a configuration of 12 rows of mirrors.

Cylindrical shaped mirrors, which present quite similar optical behavior compared with parabolic shaped mirrors, are a suitable alternative solution from a practical and financial perspective because they involve an easier and cheaper manufacturing process. The main characteristic of cylindrical mirrors is the radius of curvature, which is twice the focal length of parabolic shaped mirrors for the same receiver height (Abbas et al. 2012). A higher radius of curvature implies a smoother geometrical profile, which entails a significant advantage for the manufacturing of the concentrator because it may be accomplished with thin glass mirrors glued over a cylindrical preformed pattern, which is easy to achieve.

In LFR systems, every mirror has a singular focal distance to the receiver, which leads to a different radius of curvature for each mirror. Manufacturing different preformed pattern with every radius of curvature certainly increases the cost of the LFR. An iteration process was performed with the goal of maximizing the power impinging in the receiver while using one single radius of curvature for all mirrors. At each iteration, a specific radius of curvature was employed for all mirrors, which was changing from the focal distance of the farthest mirrors from the receiver to the focal distance of the nearest mirror. It was established that the radius of curvature of the farthest mirror delivers the best results. In addition, it was concluded that the impinging power in the receiver for this particular configuration (i.e. the radius used for all the mirrors is the one corresponding to the farthest one) is similar to the power achieved when every mirror has its own specific radius.

3.3. Point strategy

Fig. 5 shows the image form by the rays if every mirror would point to the central position in the receiver. In this approach, the rays are concentrated in the central tubes, leaving the external tubes with no rays at all. As it was explained in section 2.4, this point strategy leads to generate hot spots that are prejudicial to the overall performance of LFR.

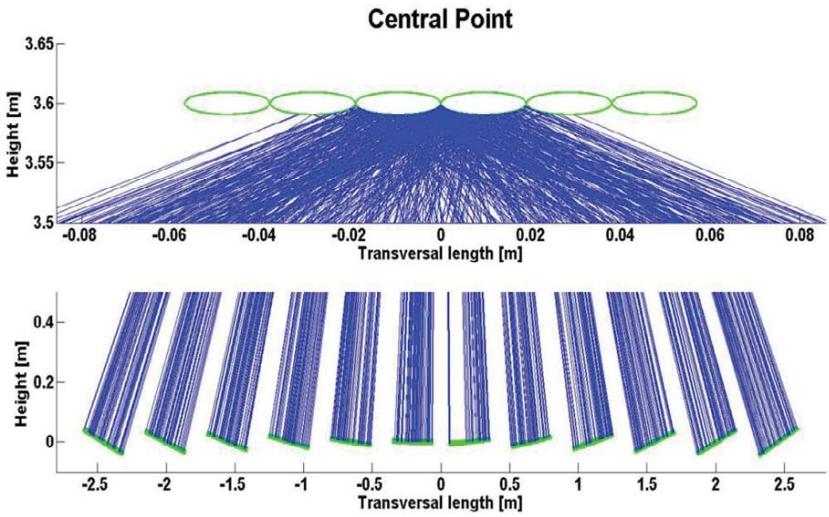

Fig. 5. Rays impinging in receiver following a central point strategy.

On the contrary, if an individual point strategy is taken into account, in which a group of mirrors aims exclusively at a specific tube, the image formed by the rays is much more homogeneously distributed, as expected. As it can be seen in Fig. 6, the power flux in the receiver is more uniform when this strategy is applied. In this figure, the red lines represent those rays missing the receiver.

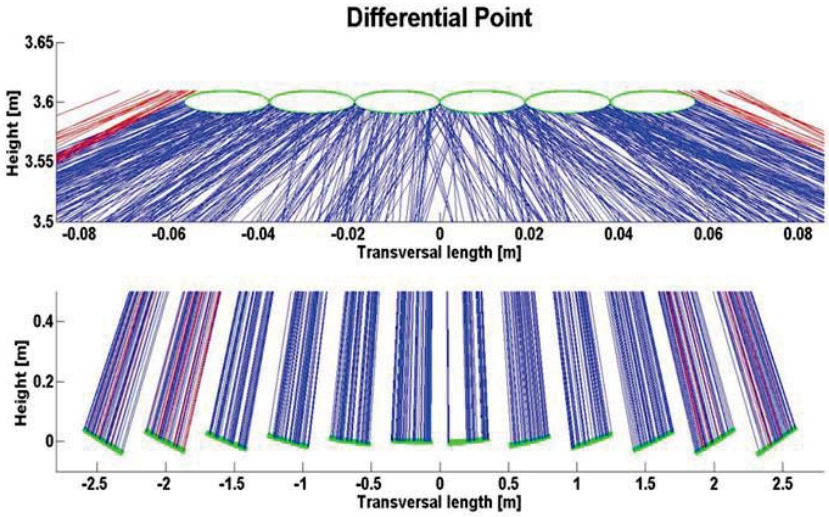

Fig. 6. Rays impinging in receiver following a differential point strategy.

The point strategy assumed in this case is based on a compromise between the concentration ratio and flux distribution.

3.4. Optimized height of receiver

Fig. 7 shows the power obtained when the height of the receiver is varied, for different number of mirror rows. Every number of rows presents one specific receiver height in which the power is maximized (indicated by the red circles in the graph). If the receiver is placed below the optimum height, blocking and shadows become predominant and consequently fewer rays reach the receiver, and therefore reducing the impinging power. On the contrary, in case of locating the receiver above the optimal position, it implies a higher rate of rays missing the target because the effect of sunshape becomes noticeable when the distance traveled by reflected rays increases. Additionally, a stochastic approach to model the deviation of rays caused by mirrors aberrations was included in the model. The longer distance traveled by the rays, the more noticeable this phenomenon is. If the receiver height is not increased after adding mirrors, the furthest one will present a pronounced tilt, which will lead to increase shadings on the neighbor mirrors and consequently a reduction in the power with respect to the corresponding optimum height for that number of mirrors. For this reason, the optimized receiver height is larger for a higher number of rows of mirrors. Finally, for the selected configuration with 12 rows of mirrors the optimal height of the receiver is 3.4 m.

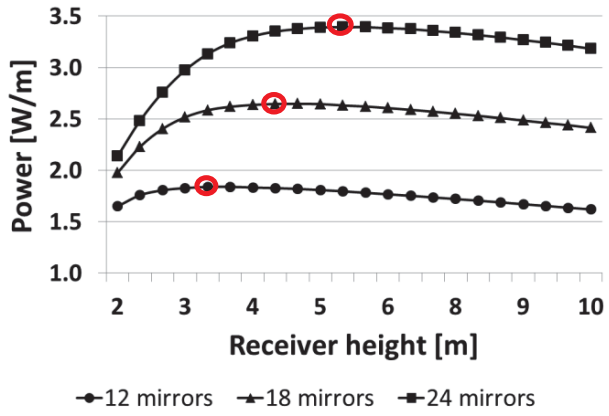

Fig. 7. Normalized power ($Power_{reference}$ = 1 Wm^{-2}) in receiver related with its height for different number of mirrors.

3.5. Number and width of mirrors

According to the methodology explained in section 2.6, the number and width of mirrors could be selected with the in-house code presented in this work, for every specific facility, by considering both the expected power and several technical, economical and practical aspects. For example, as shown in the previous section, every

mirror configuration involves an optimum receiver height, which must be suitable for the facility characteristics as well. The selected configuration is made up of 12 rows of mirrors of 0.28 m width.

3.6. Length of receiver tubes

The thermal energy model described in section 2.7 was applied. An increase of 20 ºC in the HTF temperature was set as the criterion to determine the absorber length. Such a high thermal gain was imposed in order to minimize the temperature relative errors when carrying out the experimental test campaign. The accuracy of the measurement instruments was also considered at the time of setting the temperature difference in the LFR. The length of the receiver that satisfied this condition is in the range of 10 to 12 meters.

The four heat loss correlations explained in section 2.7 were not in agreement among them. It was found a difference of up to 30% in the calculated length of the receiver. All the correlations regarded use different criterion for the definition of ΔT This disagreement could be the reason of such an inconsistent results.

3.7. Benchmarking of ray-tracing code

The optical model presented in this work was cross checked with a free ray tracer software, called Tonatiuh (Blanco et al. 2009). This software allows simulating a LFR with its geometrical and optical characteristic. The results of the comparison are showed in Fig. 8. Six charts can be seen in this figure, one for each tube in the receiver. In every chart, the normalized power impinging in the receiver is presented versus the angular coordinate around the tube perimeter (expressed in radians).

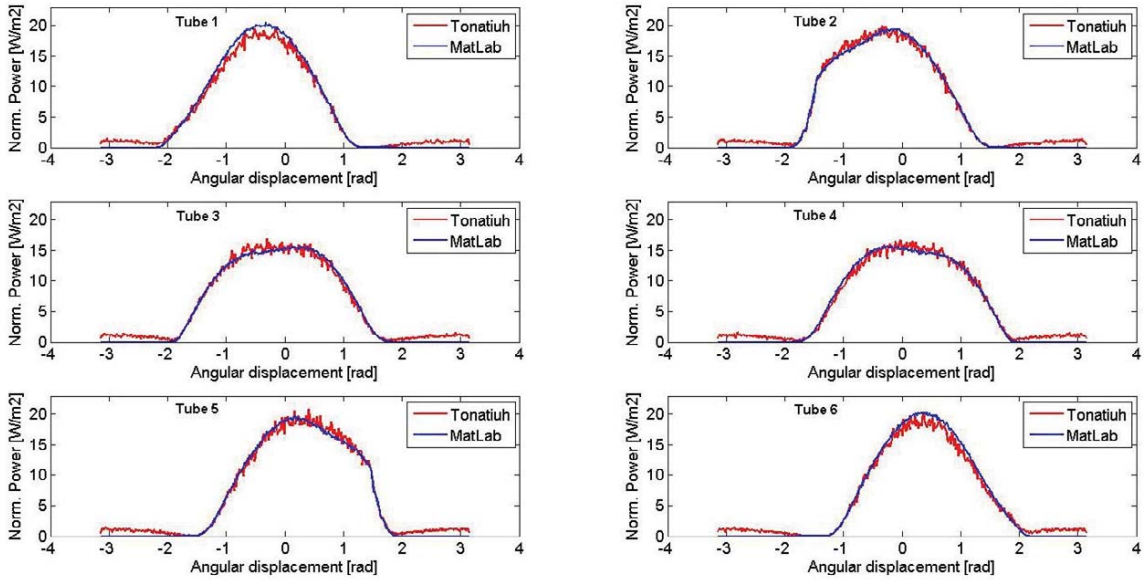

Fig. 8.Simulated normalized power impinging in receiver tubes from Tonatiuh software (red) and in-house Matlab code (blue). ($Power_{reference}$ = 1 Wm^{-2}, Location: Plataforma Solar de Almería, Spain).

For every single tube of the receiver, it was found that the curves profile and values of normalized impinging power match satisfactorily in both simulations.

4. Conclusions

A detailed design procedure for a Linear Fresnel solar collector was described. The collector was designed to provide thermal energy in IPH applications. The reflector configuration was determined by means of an in-house ray tracing code. The mirrors follow a cylindrical shape, the number of rows selected for the prototype to be built is 12 and the width chosen for each one is 0.28 m. The receiver configuration is a multitube cavity receiver composed of 6 parallel tubes and a trapezoidal cavity around 11 m long located 3.4 m over the mirrors plane. For mirrors tracking, a differential point strategy was analyzed with the objective of achieving a more homogeneous flux distribution on the multitube receiver panel. The next steps in the design process are optimizing the final design and building a prototype at the *Plataforma Solar de Almería*. Further work, can be

done from the current model, including the optimization of the mirrors shift value according to economical and technical restrictions.

5. References

Abbas, R., Montes, M.J., et al., 2012. Solar radiation concentration features in Linear Fresnel Reflector arrays. Energy Conversion and Management. 54(1), 133–144.

Abbas, R., Muñoz, J. & Martínez-Val, J.M., 2012. Steady-state thermal analysis of an innovative receiver for linear Fresnel reflectors. Applied Energy. 92, 503–515.

Blanco, M.J. et al., 2009. Preliminary validation of Tonatiuh. SolarPaces Conference.

Boito, P. & Grena, R., 2016. Optimization of the geometry of Fresnel linear collectors. Solar Energy. 135, 479-486.

Buie, D., Monger, A.G. & Dey, C.J., 2003. Sunshape distributions for terrestrial solar simulations. Solar Energy. 74(2), 113–122.

Fernandez-Garcia, A. et al., 2010. Parabolic-trough solar collectors and their applications. Renewable and Sustainable Energy Reviews. 14(7), 1695–1721.

Haeberle, A. et al., 2002. The Solarmundo line focussing Fresnel collector. Optical and thermal performance and cost calculations. Proceedings of SolarPACES, 1–11.

Incropera, F.P., 2007. Fundamentals of Heat and Mass Transfer 6th ed.

Kalogirou, S., 2003. The potential of solar industrial process heat applications. 76, 337–361.

Kumar, S., Independent, N. & Madras, T., 2012. Heat loss characteristics of trapezoidal cavity receiver for solar linear concentrating system. Aplplied Energy. 93, 523–531.

Montes, M.J. et al., 2016. Performance model and thermal comparison of different alternatives for the Fresnel single-tube receiver. 104, 162–175.

Neumann, A. et al., 2002. Representative Terrestrial Solar Brightness Profiles. Journal of Solar Energy Engineering. 124(2), 198.

Pye, J.D., Morrison, G.L. & Behnia, M., 2003. Modelling of Cavity Receiver Heat Transfer for the Compact Linear Fresnel Reflector. Manufacturing Engineering, 1–9.

Reynolds, D.J., Behnia, M. & Morrison, G.L., 2002. A Hydrodynamic Model for a Line-Focus Direct Steam Generation Solar Collector. Solar 2002, 1–6.

Sahoo, S.S., Singh, S. & Banerjee, R., 2012. Analysis of heat losses from a trapezoidal cavity used for Linear Fresnel Reflector system. 86, 1313–1322.

Sait, H.H. et al., 2015. Fresnel-based modular solar fields for performance/cost optimization in solar thermal power plants: A comparison with parabolic trough collectors. Applied Energy. 141, 175–189.

Singh, P.L., Ganesan, S. & Yàdav, G.C., 1999. Performance study of a linear Fresnel concentrating solar device. Renewable Energy. 18(3), 409–416.

Singh, P.L., Sarviya, R.M. & Bhagoria, J.L., 2010. Heat loss study of trapezoidal cavity absorbers for linear solar concentrating collector. Energy Conversion and Management. 51(2), 329–337.

Zhu, G. et al., 2014. History, current state, and future of linear Fresnel concentrating solar collectors. Solar Energy. 103, 639–652.